



ÓBUDAI EGYETEM  
ÓBUDA UNIVERSITY

DOCTORAL SCHOOL OF MATERIAL  
SCIENCES AND TECHNOLOGIES

Doctoral (PhD) theses

# Investigation and application of particle and cell separation methods in microfluidic systems

Anita Bányai

Supervisor: Dr. Péter Fürjes

Industrial consultant: Máté Varga

Budapest, December 2024.

HUN  
REN



Energiatudományi  
Kutatóközpont



77 ELEKTRONIKA

## I. History of the research

---

In the field of microfluidics, the development of medical diagnostic applications has received great emphasis in recent decades with special focus on Lab-on-a-chip (LOC) or miniaturized total analytical ( $\mu$ -TAS) systems, Point-of-Care (POC) diagnostic platforms, which can be used at the patient's bedside, ambulances or medical offices. The Covid-19 pandemic also served as a catalyst for the spread of self-testing platforms: from 2019 to 2020 the global market for in-vitro diagnostics (IVD) achieved annual growth of 25.2% [1]. Checking the blood sugar level, identifying the stage of a heart attack, stroke, and detecting rapid bacterial and viral infections require accurate and immediate measurement results. That is why the requirements against the microfluidic devices used in medical diagnostics are achieving fast, efficient and reliable analytical results in a short period of time, even from samples with a volume of a few nano- or microliters, which can support medical decision-making about further necessary treatments.

Related to the development of the Rapid Urine Bacteria Analyzer (RUBA) system of 77 Elektronika Ltd., the need arose for a consumable, which is suitable for appropriate sample transport, sample preparation as target separation, enrichment, and lateral positioning in the sensor zone. In urine various elements can be found from the squamous cells with a typical diameter of 60  $\mu\text{m}$ , through particles with various shapes and sizes (crystals, fungi, hematopoiesis), even bacteria with a size of 1 - 4  $\mu\text{m}$ . The advantage of the primarily examined label-free cell separation methods is that it can be performed without choosy sample preparation, and the segregability is based on the variety of the physical parameters of the cells - size, shape, density, flexibility, polarizability.

The separation methods can be classified in two groups: active separation methods require the involvement of external resources: including magnetic, acoustophoretic, dielectrophoretic and optical solutions; or the passive segregation methods that do not require an external resource, but require more careful geometric

design: as in case of Deterministic Lateral Displacement (DLD), Micro vortex manipulation, Inertia and Dean flow separation options, Filtering or others.

Each method has the advantages and the disadvantages considering the specifications of the application and its defining parameters. Dielectrophoretic separation is capable of real-time focusing with high resolution, however, its disadvantages include the high conductivity of the medium and the fragility of biological samples. The advantage of magnetic separation is the almost highest throughput among active separation methods: microfluidic solutions have already appeared in clinical applications that were able to extract E.coli from 50-100 ml of sample in 15 minutes [2], or bind sepsis-causing bacteria at a concentration of 10 CFU/ml [3]. Among the research groups' strategic approaches aimed at increasing efficiency are the optimization of the geometry of the fluidic channel, the surface treatment or the size of the target-specific magnetic beads.

The advantage of passive separation methods is that the filtering is optimized for a property of the used medium or target.

1) **Deterministic Lateral Displacement (DLD)** is a label-free method for separation and segregation cells or enrichment of target populations. It is based on a row-by-row shifted column system, in which the degree of periodicity and the size of the column spacing determine the critical particle diameter ( $D_c$ ), above which the particles are deflected. Huang et al. [4] laid the foundation for the method for DLD system with circular columns. One of its challenges is the limited segregation of non-spherical, deforming entities, which can continuously change their shape and form of movement in the flow as they approach the columns. The method is suitable for separating healthy - more flexible - and malaria-infected - more rigid - red blood cells [5], and the size-dependent segregation method also works in the sub-micron range.

2.) **Cross-flow filtration (CF)** is a pressure-controlled membrane process, which is also suitable for separating fine particles, microorganisms, and emulsion droplets. In contrast to dead-end filtration processes, in this solution the surface of the

filter is located parallel to the liquid flow, which significantly reduces the possibility of clogging. CF technology is usually used in combination with another separation process. Comparing the efficiencies of the filtration procedures found in the literature are difficult due to the different pore sizes, filtration time, sample composition and concentration, and the degree of biofouling formed on the filter. Regarding the geometry of the microfluidic filter: between columnar or weir-type arrangements, the second one shows more effective filtration [6] at a flowrate of 10  $\mu\text{l}/\text{min}$  and a concentration of  $10^4$  cells/ $\mu\text{l}$ : efficiency of 82.3% was achieved with the column type and 91.2% with the weir - type arrangement during the separation of red blood cells. My tests also covered these filter types.

3.) **Lateral focusing** is a continuous and high-throughput method, and in terms of its function, it arranges homogeneously distributed particles in a laminar manner in a single flow line by exploiting inertial lifting forces. The particle size, the channel geometry, its cross-section and the flow Reynolds number also influence the focal points of the particles' position in the cross-section of a microfluidic channel. During my experiments study of Dino Di Carlo et. al. [7] was considered, in which the focusing criteria of fluidics was defined in an asymmetric serpent channel ( $a/D_h > 0.07$ ) with regard to the ratio between the particle size ( $a$ ) and the hydrodynamic diameter ( $D_h$ ) of the channel. Counter-rotating Dean vortices in the channel cross-section can promote or deteriorate the degree of focusing. Particles of different sizes occupy different equilibrium positions in the flow. The shearing force acting on the particles significantly influences their form of movement in the channel, for this reason I also investigated the lateral focusing of several biological targets (Red Blood Cells, *Escherichia coli*, *Saccharomyces cerevisiae*, HeLa cells) in comparison with the behavior of polystyrene beads. The method was used to filter cancer cells, to separate hematopoiesis or bacteria, also in the case of samples that behave as non-Newtonian fluids (milk, undiluted blood).

## II. Objectives

---

During my research work, particle separation solutions were investigated that can be implemented in a microfluidic system and operate on the principle of passive and active manipulation. In terms of the application of the developed and tested structures, an important aspect was the ability of integration into the further diagnostic system, the portability. Other prominent aspects of the design are the geometrical and material properties of the microfluidic system considering the parameters of the target cells. During the development of the RUBA (rapid urine bacteria analyzer), i.e. rapid urinary tract bacteria analysis measuring device, the direct goal was to filter bacteria ( $\text{Ø} < 4 \text{ }\mu\text{m}$ ) and position them in the flow.

Accordingly, microfluidic sample preparation structures were developed that are suitable for filtering and separating shaped elements that are outside of the size range of bacteria and that may influence subsequent measurement tasks, and provide the possibility of concentrating shaped elements of different sizes in the sensor area. The basic parameters of the separation processes and structures were designed mainly considering the size restrictions, therefore the permeability, efficiency, robustness, combinability and integrability of the chosen solutions were also taken into account. In the case of the developed microfluidic units, their performance depending on the geometric parameters was examined, and a proposal was made for the optimal morphological and operational parameters.

In my study, passive separation solutions were investigated based on hydrodynamic principles, such as **(1) deterministic lateral displacement (DLD)**, **(2) lateral focusing (LF)** and **(3) crossflow filtration (CF)**, as well as **active (4) magnetic trapping** separation efficiency and their integrability.

### III. Test methodes

---

**1. Production of microfluidic systems.** Microfluidic systems suitable for laboratory experiments were produced using soft lithography [8] methods. The geometric designs was drawn with the help of mask design software (ClewIn5), based on which the chrome masks of the pattern were created by direct writing (Heidelberg DWL 66). For the optical lithography, the SU-8 negative photoresist layer was applied to a 4-inch silicon wafer in a layer thickness corresponding to the height of the desired fluidic channel, and then the negative pattern of the microfluidic system was crosslinked on it. Polydimethylsiloxane (PDMS) polymer (Sylgard 184) was used that can be mixed from two components for replica molding. For the leak-free connection of the hybrid PDMS-glass microfluidic device, oxygen plasma surface treatment was used, which promotes the formation of the covalent bond. In fluidics, the continuous flow was ensured with an RS232 ADDR syringe pump.

**2. Fluorescent studies.** For the measurements, a Zeiss Axio Vert.A1 fluorescence microscope was used, equipped with a high-sensitive cameras (Zeiss Axio IC m1; Zeiss Axio 512 mono). During the examination of lateral focusing, the images taken by a long exposure time, enabled the examination of the trajectories of fluorescent beads of different sizes and the determination of their lateral position, thus the real-time observation of the process of particle separation, target enrichment, and filtration. By choosing a unique emission wavelength for each of the fluorescent polystyrene beads of various sizes, it was possible to observe them together and to detect their presence in the filtrate. In the case of biological samples without fluorescent labeling, dark field images were taken. The images recorded at the given wavelength can also be displayed together with coloring in the ZEN 2.6 (Blue Edition) software.

**3. Evaluation.** To evaluate the recordings, Image J 1.52a software was used with various extensions, which is suitable for (1) evaluating contact angle measurements, (2) detecting the dilution of fluorescent solution based on the pixel intensity, and (3) determining the number of beads found in a given area on a fluorescent, grayscale image based on the bead size and pixel number.

During the examination of the cross-flow filtration and the magnetic trapping, the composition of the particle solutions and the filtrate was determined, as well as their cellular concentration, in the classical way, by counting them in a Bürker chamber. To automate the counting, a LUNA-II cell counter was used based on digital microscopy (Logos Biosystems) with compatible C-Chip (DHC-N01 – Neubauer Improved) cell counting chambers.

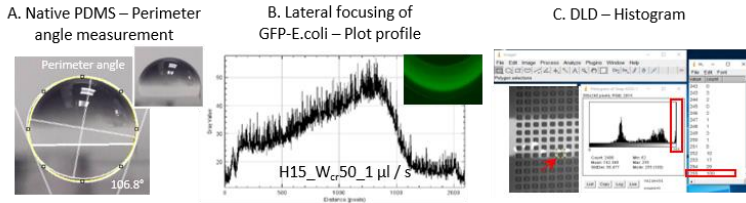


Figure 1. Application of Image J software extensions

For the experiments, fluorescent polystyrene beads of different sizes ( $\text{Ø} = 0.5 - 20.4 \mu\text{m}$ ) were used, among the biological samples of different shapes and sizes were GFP-expressing *E. coli*, red blood cells, *Saccharomyces cerevisiae* yeast cells, and HeLa cells from a cancer cell line. For the magnetic measurement, in addition to a neodymium magnet,  $\text{Ø} = 2.8 \mu\text{m}$  Dynabeads beads were used.

The experimental results were also compared to finite element models (COMSOL Multiphysics) during the investigation of lateral focusing and magnetophoretic trapping. Using numerical methods, the effects of the channel cross-section and the flow velocity were analyzed on the formation of the developing Dean vortices, as well as their effect on the lateral positions of the beads having different diameters in the channel cross-section and on the bead distribution. The measured lateral positions of the fluorescent beads were compared to the simulated Poincaré maps featured by similar parameters set. Regarding the investigation of the trapping of magnetic beads, the effects of the evolving velocity field around complex microstructures were characterized and the definition of trapping zones were supported by the results of finite element simulations.

## IV. New scientific results

---

### IV.1 Deterministic lateral displacement

**DLD (deterministic lateral displacement)** During the DLD experiments, the parameters of the column system was designed on the basis of a predefined cut-off value ( $D_c = 13.3 \mu\text{m}$  for circular columns). The shape and configuration of the pillars affect not only the particle separation effect, but also the flow characteristics experienced in laminar flow. The  $D_c$  value can be adjusted by the width of the stream lines formed between the columns. The effect of the column shape on the separation phenomenon was investigated, as well as the factors affecting efficiency arising from the resulting flow anisotropy phenomenon. To interpret the experimental results, a finite element model was built, which supports the empirical order of the separation efficiency by determining the velocity profile formed inside the column gaps – taking into account the location and value of the velocity maxima. Using the DLD microfluidic systems containing symmetric (square-based) and asymmetric (differently oriented right-angled triangle-based) columns, the effects of the emerging flow conditions on particle deflection was investigated.

#### I.1. THESIS

By comparing the separation efficiency of DLD microfluidic structures in case of six different column geometries (square, circle, triangle and right-angled triangle columns with different orientations), it was found that the velocity and pressure distribution between the columns significantly affects the trajectories of the particles in the column matrix - thus modifying the theoretical critical diameter ( $D_c$ ) characterising the arrangement. Among the designed DLD structures featured by a column distance of  $90\mu\text{m}$  and a gap size of  $40\mu\text{m}$ , as well as a displacement parameter of  $2.86^\circ$ , the one with symmetrical square-based columns gives the best  $\sim 1000\mu\text{m}$  separation deviation for the investigated particles having a diameter of  $20.4\mu\text{m}$ , considering 20 column periods . (see Figure 2)

Scientific Publication Po3



## I.2. THESIS

It was found and demonstrated through the behavior of *E. coli* bacteria that the asymmetric velocity field induced by columns with a strong orientation (e.g. based on a right-angled triangle) significantly modifies the trajectories of the particles, thereby degrading the separation efficiency of lateral migration. In DLD microfluidic systems containing asymmetric columns (based on right-angled triangles with different orientations) characterized by the specified geometrical parameters, the lateral extent of the sample solution widens to 255 - 363% of its input, focused value, so that the shaped elements are not separated from this range.

(see Figure 3.)

Scientific publication Po3

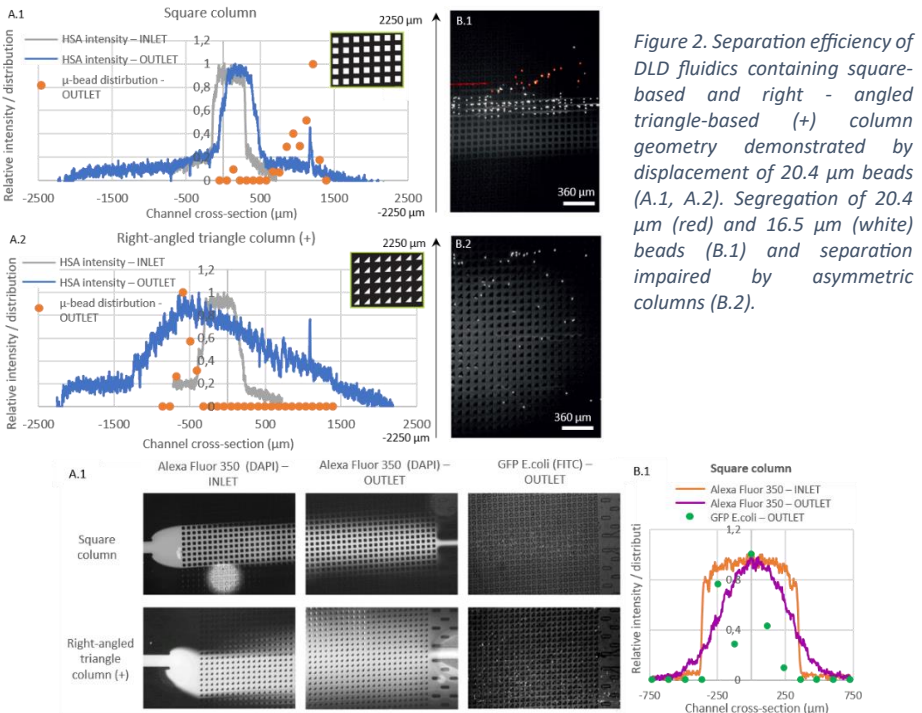


Figure 2. Separation efficiency of DLD fluidics containing square-based and right - angled triangle-based (+) column geometry demonstrated by displacement of 20.4 μm beads (red) and 16.5 μm (white) beads (B.1) and separation impaired by asymmetric columns (B.2).

Figure 3. Flow conditions in DLD structures containing square-based and asymmetric right-angled triangle-based columns. A target below  $D_c$  (critical diameter) (GFP-*E.coli*;  $\phi=0.5-2 \mu\text{m}$ , rod-shaped) moves in the column system without being transferred from the Fluorescent Alexa Fluor solution. The flow field created due to the asymmetric column structure significantly widens the target distribution in the microfluidic system.

## IV.2 Crossflow filtration

During my experiments (1) in the case of a crossflow filter structure, the separation efficiency of the microfluidic system was characterized as the function of the height ratio of the filter channels and the main flow channels. In each case, the microfluidic system consists of a 500  $\mu\text{m}$  wide main channel and two 200  $\mu\text{m}$  wide side channels, as well as the parallel filter structure formed between them; the inlet volumetric flow rate was 0.5  $\mu\text{l/s}$ . (2) In the case of the weir-type filter structure, the effect of the hydrodynamic resistances of the main and side channels on the filtration efficiency was investigated - which was achieved by changing the width of the main channel (500 / 300  $\mu\text{m}$ ) and the height of the side channel (50 / 25  $\mu\text{m}$ ), with the same 5  $\mu\text{m}$  filtration gap. In my experiments, the typical sizes of the applied model particles were chosen to be similar to the shaped elements in urine (E. coli – 1.97  $\mu\text{m}$ , red blood cells – 6.08  $\mu\text{m}$ , white blood cells – 15.8  $\mu\text{m}$ ). The sensitivity of the filtration process to the cross-flow rate, the transmembrane pressure, the hydrodynamic resistance of the membrane and the resulting compaction layer, and the size distribution of the particles in the suspension was investigated.

### II.1. THESIS

It was found that structures with a larger (filter channel / main channel) height ratio are better in terms of filtration efficiency: in addition to extracting a similar amount of target particles, the passage of larger particles can be significantly reduced, and the purity of the filtrate can be improved. The number of particles with a diameter of 6.08  $\mu\text{m}$  appearing next to particles with a diameter of 1.97  $\mu\text{m}$  was reduced by 79.5% and 69.6%, respectively, in structures with a height ratio of 1:10 (5 $\mu\text{m}$  / 50 $\mu\text{m}$  and 10 $\mu\text{m}$  / 100 $\mu\text{m}$ ), compared to those with a height ratio of 1:5 (5 $\mu\text{m}$  / 25 $\mu\text{m}$  and 10 $\mu\text{m}$  / 50 $\mu\text{m}$ ).

(see Figure 4.A)

Scientific publication: Po2

### II.2. THESIS

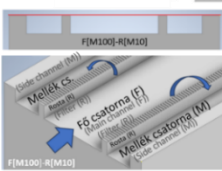
It was found that with a constant mass flow, the efficiency of the filtration is deteriorated due to the increased local flow velocity in the main channels having a smaller cross-section. It was proven that the weir-type cross-flow filter tested as a passive separation structure is suitable for pre-filtering small cells, E. coli bacteria; however, the effectiveness of the filtration depends on the presence of non-specific shaped elements in the sample. In the case when 6.08  $\mu\text{m}$  and 15.8  $\mu\text{m}$  diameter beads

mixed into the sample, the yield of filtered *E. coli* bacteria decreased by ~35%. Due to elements larger than the filter size, the filtration compaction layer formed on the filter surface significantly hinders the passage of target cells into the filtrate. (see Figure 4.B)

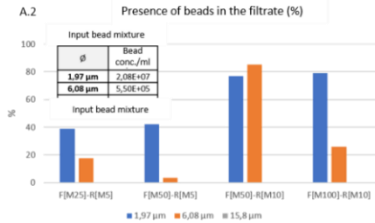
Scientific publication: Po2

### A. Cross-channel filtration

A.1

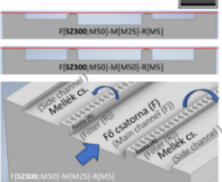


A.2

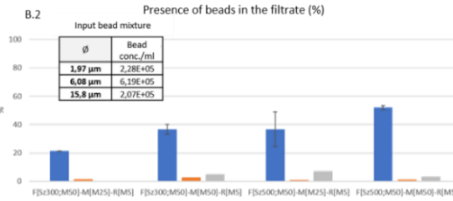


### B. Weir-type filtration

B.1



B.2



### b. weir-type filtration – *E. coli* vs. beads and *E. coli*

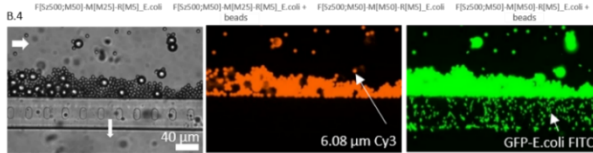
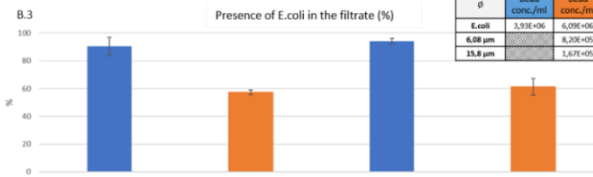


Figure 4. The efficiency of the filtration in an arrangement containing cross channel filter (A.) or a weir-type filter (B.). Filtration efficiency experienced in different geometries (A.1-B.1) with the same bead sizes:  $\phi$  15.8; 6.08; 1.97  $\mu\text{m}$ . *E. coli* can be detected in the filtrate (B.3) in case of samples without (blue) and with additional beads (orange) in a weir-type arrangement featured by F[W500;M50] main channel dimensions, or M[M50] and M[M25] side channel heights. The filtration cake formed on the surface of the filter (B4.).

### IV.3 Lateral focusing

In a microfluidic channel with a periodically changing cross-section, made up of asymmetric bends the effect of the geometric parameters of the channel on the separation efficiency of particles of different sizes were investigated. The hydrodynamic processes was interpreted using a finite element model, identifying the focusing effect of the more elongated Dean vortices formed in the microfluidic system. The applied fluidic unit consisted of 23 bends; channel heights and critical cross sections were chosen to be between  $H = 100, 50, 25, 15 \mu\text{m}$  and  $W_{cr} = 50, 100, 150 \mu\text{m}$ , respectively. In accordance with the targeted biological applications, the microfluidic system was optimized for the positioning of beads with a diameter of  $15.8$  and  $4.8 \mu\text{m}$ , at flow rates of  $0.5 - 1 - 3 - 5 - 6 \mu\text{l/s}$ . The experimental results were compared to the numerical results of finite element modeling, highlighting the effects of the channel cross-section and the flow velocity on the behavior of the emerging Dean vortices. The lateral position and distribution of beads of different diameters were analysed in the channel cross-section considering their Y coordinates determined by trajectory calculations.

It was examined in a dedicated structure characterized by channel parameters  $H=25 \mu\text{m}$  and  $W_{cr}=50 \mu\text{m}$ , how accurately the recorded model bead position map can represent the behavior of the selected biological cells: *E. coli* [ $0.5\text{-}2 \mu\text{m}$ ; stick], red blood cell [ $2.5$ ;  $6\text{-}8 \mu\text{m}$ ; disc-shaped biconcave], yeast *Saccharomyces cerevisiae* [ $5\text{-}10 \mu\text{m}$ ; round or oval] and HeLa cell line [ $16\text{-}29 \mu\text{m}$ ; varied, inhomogeneous, sphere in suspension], which differ not only in size but also in shape. To set up the position map, the following bead sizes were used in the experiments:  $\emptyset = 0.5 - 1.1 - 1.97 - 2.9 - 4.8 - 5.4 - 6.08 - 10.2 - 15.8 - 16.5 \mu\text{m}$ . The further focusing of *E. coli* bacteria were investigated in  $25$  and  $15 \mu\text{m}$  high channels. The difficulty of focusing is due to the fact that *E. coli* is rod-shaped, the smallest dimension is  $0.5 \mu\text{m}$ , the largest is around  $2 \mu\text{m}$ , and they are much more deformable than polystyrene beads.

The experiments were also supported by simulations revealed that the efficiency of focusing can be improved by increasing the flow velocities, reducing the channel cross-section, or increasing the channel length and the number of periods. In addition, the sensitivity of the applied biological target to shear forces must be taken into account, as well as the permeability of the channel, or the possibilities of miniaturization - when using a long channel geometry.

### III.1. THESIS

It was found that by reducing the height of the channel ( $50\ \mu\text{m} \rightarrow 25\ \mu\text{m}$ ), the efficiency of focusing smaller beads and the separation of the size dependent particle positions can be significantly improved. In the most efficient microfluidic channel with the height of  $H=25\ \mu\text{m}$  and the critical cross section of  $W_{\text{cr}} = 50\ \mu\text{m}$ , at the volume flow rate of  $1\ \mu\text{l/s}$ , using particles with diameters of  $15.8$  and  $4.8\ \mu\text{m}$ , the distance between their lateral focus positions can achieve the 20 % of the output cross-section.(see Figure 5.)

Scientific publication P2, P3

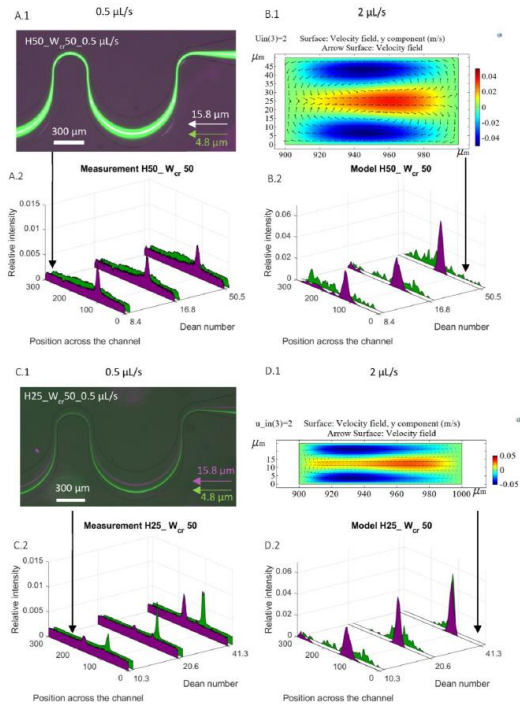


Figure 5. Illustration of the behavior of rigid polystyrene beads ( $\varnothing 4.8$  and  $15.8\ \mu\text{m}$ ) in  $H50\_W_{\text{cr}}50$  and  $H25\_W_{\text{cr}}50$  fluidic channels with different critical cross-sections at flow rates of  $0.5 - 1 - 2\ \mu\text{l/s}$  (corresponding Dean numbers). Experimental results: detection of the bead positions at the output, based on fluorescence intensity (A.1 – A.2 and C.1 – C.2). The results of the numerical simulations illustrate the distribution of the velocity field in the  $x$ - $y$  plane in the smaller bend of the channel ( $W_{\text{cr}} + 50\ \mu\text{m}$ ) at a flow rate of  $2\ \mu\text{l/s}$  (B.1, D.1), as well as the lateral distribution of the beads (taken on the  $y$  axis) 23 bends after (B.2, D.2).

### III.2. THESIS

It was proven by experimental results that the concentration efficiency of the target *E. coli* bacteria can be improved by significantly reducing the height in the microfluidic channel containing periodic bends with asymmetrically changing cross-sections. In the microfluidic channel with the height of 15  $\mu\text{m}$ , at a flow rate of 1  $\mu\text{l/s}$ , the cell population was concentrated on 77% of the cross section of the 300  $\mu\text{m}$  wide channel.

(see Figure 6.)

Scientific publication P2, P3

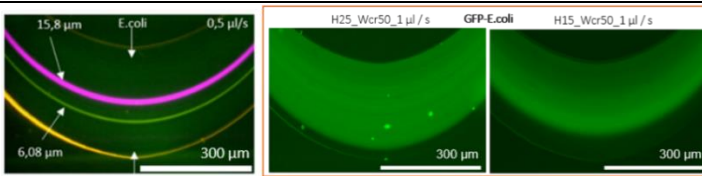


Figure 6. The degree of concentration of *E. coli* in a microfluidic channel containing periodic bends with asymmetrically changing cross-section at flow rates of 0.5 and 1  $\mu\text{l/s}$ . Greater concentration of *E. coli* was achieved by reducing the height of the channel.

### III.3. THESIS

Taking advantage of the periodicity of the applied microfluidic system, a cyclically repeating finite element model was proposed, whose output parameters (velocity field, particle trajectories) were again defined on the input boundary, accordingly the behavior of a microfluidic system of arbitrary length can be modeled with moderate resource demand, without having to manufacture, just by defining its digital twin. Examining and comparing the flow behavior of target cells and polystyrene beads in a manufactured fluidic system, the rigid sphere diameters were determined, which present equivalent characteristics to *E. coli*, red blood cells, yeast and HeLa cells of various morphologies: 1–2  $\mu\text{m}$ , 5–6  $\mu\text{m}$ , 10  $\mu\text{m}$ , 15–17  $\mu\text{m}$ . By comparing the numerical results of the finite element simulations with the experimental results, the model was found to give good results regarding the lateral position, but can only calculate its distribution with a larger margin of error.

(see Figure 7.)

Scientific publication: P1

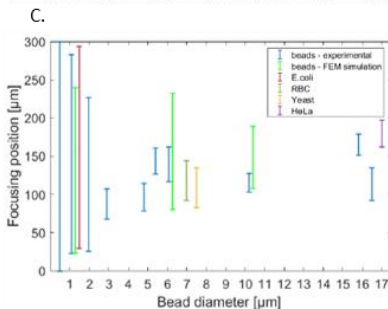
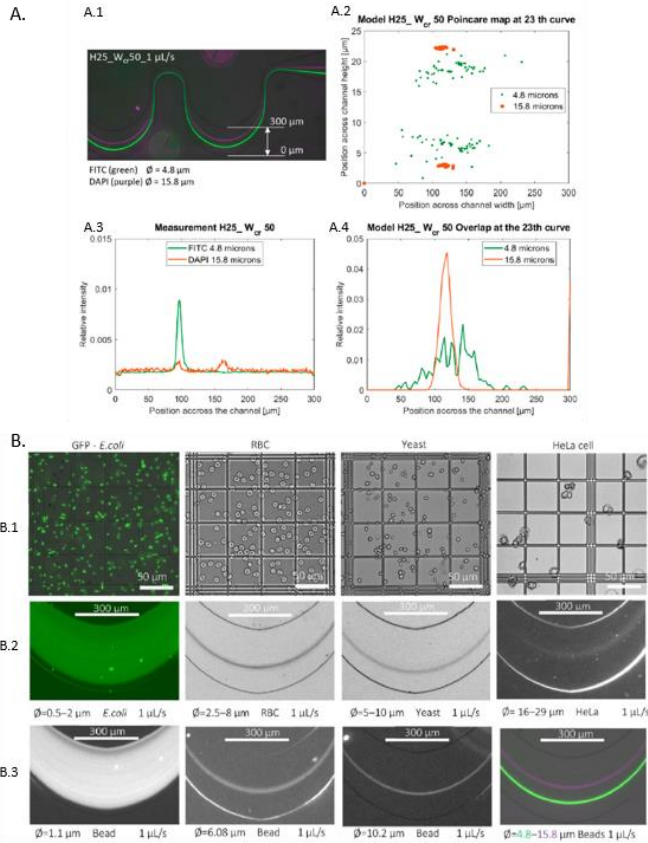


Figure 7. Comparison of experimental and finite element simulation results in H25\_Wr50 channel at a flow rate of  $1 \mu\text{L/s}$ . Experiments: trajectories of  $\phi = 4.8 \mu\text{m}$  (green) and  $15.8 \mu\text{m}$  (purple) beads (A.1) and their lateral distribution at the end of the fluidic channel (A.3), characterized by the fluorescence intensity profile. The FEM simulations:

bead distribution in the cross-section of the channel (A.2 – Poincaré map), which can be mapped to the lateral distribution (A.4). Comparison of the lateral focusing of biological cells (B.1 – B.2) and polystyrene beads (B.3): the equivalent bead size used for modeling a biological sample was determined by overlapping the lateral focusing position. Focusing position map for rigid polystyrene beads of different sizes and biological target cells (C); the simulated lateral positions of beads with various sizes also shown in the graph.

## IV. Magnetic separation

The microfluidic morphology and flow rate dependence of the magnetic trapping efficiency was characterised by experimental measurements and finite element simulations also. The behavior of the magnetic microbeads was investigated under different flow conditions, aiming to achieve the highest possible trapping efficiency. In case of the implementation of target filtering tasks, the primary consideration is to ensure high throughput and efficiency, however, increasing the flow rate worsens the trapping efficiency of the target in many cases. Geometrical inhomogeneities were prepared in the microfluidic system, which can improve the trapping efficiency by local modification of the flow field even in the case of higher global flow rates. The experimental results were compared to the results of FEM simulation. The proposed local trapping solutions were also used in autonomous microfluidic systems.

### IV.1. THESIS

It was found that the local reduction of the flow rate and the modification of the flow profile were suitable for increasing the efficiency of magnetic trapping. It was proven that around microstructures where the path taken by the particles increases - for example, due to the formation of transverse or swirling trajectories - the particles were trapped to a greater extent on the lower surface of the channel.  
(see Figure 8.)

Scientific publication: Po1

### IV.2. THESIS

By constructing a finite element model, it was shown that the numerically calculated velocity field is suitable for predicting the trapping position and local trapping efficiency of magnetic particles - therefore, the model is suitable for applying magnetophoretic separation structures as a digital twin.

(see Figure 9.)

Scientific publication: Po1



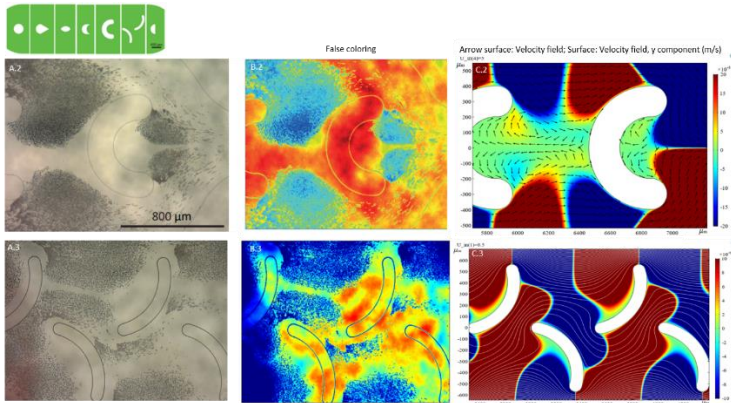


Figure 8. Magnetic trapping of microbeads in fluidics with  $25\ \mu\text{m}$  height, at a flow rate of  $1\ \mu\text{l/s}$  (A): around turned U and periodic arc shaped columns. False coloring of the recordings of the experiments: blue – trapped beads, red – absence of beads (B). Flow velocity distribution around the structures calculated by a finite element modelling (C.); according to the y component of the velocity field, blue - downward, red - upward velocity fields for the turned U (C.2) and periodic arc-shaped columns (C.3).

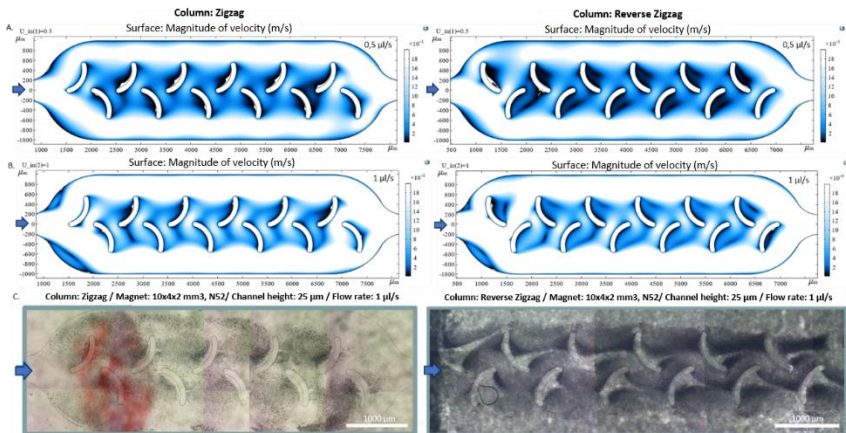


Figure 9. Effect of the orientation of and periodic arc shaped columns on the trapping distribution of magnetic beads. The initial flow velocity around the  $25\ \mu\text{m}$  high microstructures was  $0.5\ \mu\text{l/s}$  (A.), and  $1\ \mu\text{l/s}$  (B.). The expected trapping distribution on the basis of the flow velocity distribution largely corresponds to the experimental results, which was experienced in the  $25\ \mu\text{m}$  high channel at a flow rate of  $1\ \mu\text{l/s}$ . (C)

## V. The possibility of utilizing the results

---

The primary task of microfluidic cassettes is to detect the analyte to be measured (such as bacteria, protein, virus, DNA, RNA, etc.) from a sample (e.g. blood serum, urine, drinking water, etc.) with the highest possible accuracy and sensitivity, although the analyte and the other elements possibly interfering in the measurement (cells, debris, etc.) should be separated from each other. From the application aspects, these are developed for diagnostic or monitoring tasks, mostly for medical purposes, where it is important to solve the measurement with a minimum sample volume in the shortest possible time. LOC devices therefore integrate sample analysis subsystems that can trigger a series of complicated laboratory operations and carry out the measurement at the point of care. The particle or analyte separation and concentration procedures are one of the most challenging functions of the microfluidic sample preparation steps.

Examining the results from the application aspects, it can be stated that the passive separation and concentration techniques can be used in cases where the operation of the microfluidic cassette is ensured by a pressure-controlled external pump (syringe, peristaltic, piezo, other) and the increased flow rate is not critical considering the measurement method. It can be applied in other cases, where there is a dedicated sensor zone in the microfluidic cassette, but the interaction between the analyte and the recognition agent is so strong that the increased flow rate does not significantly reduce the sensitivity of the system. However, there are also many application cases where the increased flow rate can cause a significant disadvantage and a significant decrease in sensitivity. The advantage of autonomous microfluidic systems from a clinical point of view is that there is no fluidic connection between the cassette and the instrument, so the cassette forms an independent closed unit that can be disposed after measurement, however, the precise adjustment of the surface tensions, and ensuring their stability over time are critical. Providing contamination-free production of the fluidic system is also a challenge.

Definition of the optimal technology in case of a given use-case is primarily determined by the clinical needs, and secondly by the system under development. My research supports this decision, in the case of certain, frequently examined micrometer size or larger targets (bacteria, red blood cells, yeast, HeLa cells), when these passive or active separation solutions are appropriate along the given system settings.

## VI. List of literature references

---

- [1] „In vitro Diagnostics Market Size, Share & Trends, 2029”. Elérés: 2023. május 9. [Online]. Elérhető: <https://www.fortunebusinessinsights.com/industry-reports/in-vitro-diagnostics-ivd-market-101443>
- [2] K. Y. Castillo-Torres, E. S. McLamore, és D. P. Arnold, „A High-Throughput Microfluidic Magnetic Separation ( $\mu$ FMS) Platform for Water Quality Monitoring”, *Micromachines*, köt. 11, sz. 1, Art. sz. 1, jan. 2020, doi: 10.3390/mi11010016.
- [3] A. L. K. Lopes és *mtsai.*, „Development of a magnetic separation method to capture sepsis associated bacteria in blood”, *J. Microbiol. Methods*, köt. 128, o. 96–101, szept. 2016, doi: 10.1016/j.mimet.2016.07.012.
- [4] L. R. Huang, E. C. Cox, R. H. Austin, és J. C. Sturm, „Continuous Particle Separation Through Deterministic Lateral Displacement”, *Science*, köt. 304, sz. 5673, o. 987–990, máj. 2004, doi: 10.1126/science.1094567.
- [5] T. Krüger, D. Holmes, és P. Coveney, „Deformability-based red blood cell separation in deterministic lateral displacement devices-A simulation study”, *Biomicrofluidics*, köt. 8, jún. 2014, doi: 10.1063/1.4897913.
- [6] „Microfluidic chip for blood cell separation and collection based on crossflow filtration | Request PDF”, ResearchGate. Elérés: 2020. június 17. [Online]. Elérhető: [https://www.researchgate.net/publication/223530285\\_Microfluidic\\_chip\\_for\\_blood\\_cell\\_separation\\_and\\_collection\\_based\\_on\\_crossflow\\_filtration](https://www.researchgate.net/publication/223530285_Microfluidic_chip_for_blood_cell_separation_and_collection_based_on_crossflow_filtration)
- [7] D. Di Carlo, D. Irimia, R. G. Tompkins, és M. Toner, „Continuous inertial focusing, ordering, and separation of particles in microchannels”, *Proc. Natl. Acad. Sci.*, köt. 104, sz. 48, o. 18892–18897, nov. 2007, doi: 10.1073/pnas.0704958104.
- [8] Y. Xia és G. M. Whitesides, „Soft Lithography”, *Annu. Rev. Mater. Sci.*, köt. 28, sz. 1, o. 153–184, 1998, doi: 10.1146/annurev.matsci.28.1.153.

## VII. Scientific publications related to theses

---

### VII.1 Publications

- P1 Bányai, Anita ; Farkas, Enikő ; Jankovics, Hajnalka ; Székács, Inna ; Tóth, Eszter L. ; Vonderviszt, Ferenc ; Horváth, Róbert ; Varga, Máté ; Fürjes, Péter **Dean-Flow Affected Lateral Focusing and Separation of Particles and Cells in Periodically Inhomogeneous Microfluidic Channels** SENSORS 23 : 2 Paper: 800 , 19 p. (2023); <https://doi.org/10.3390/s23020800> Sensors - Q1; IF 3.9; Number of references: 1 (Independent)
- P2 Bányai, Anita ✉; Tóth, Eszter Leelőssyné; Varga, Máté; Fürjes, Péter **Geometry-Dependent Efficiency of Dean-Flow Affected Lateral Particle Focusing and Separation in Periodically Inhomogeneous Microfluidic Channels**, SENSORS 22 : 9 Paper: 3474 , 13 p. (2022); <https://doi.org/10.3390/s22093474>; Sensors - Q1; IF 3.9; Number of references: 1 (Independent); 1 (Dependent)

- P3 Bányai Anita, Bató Lilia, Leelőssyné Tóth Eszter, Varga Máté, Fürjes Péter\*  
**Áramlástan j elenségek mikroszkopikus mérettartományban – mikrofluidikai**; Fizikai Szemle

## VII.2 Conference appearances

- Po1 Anita, Bányai; Eszter, Leelőssyné Tóth; Péter, Fürjes; **Effect of channel morphology on magnetic separation in microfluidic particle trapping** (2022) SelectBio, Lab-on-a-Chip and Microfluidics Europe 2022, Rotterdam 2022, 20.06.2022. (June 20-21, 2022.)
- Po2 Anita, Bányai ; Máté, Varga ; Péter, Fürjes; **Filtration efficiencies of crossflow type microfilters for E.Coli separation** (2022) Mátrafüred International Meeting on Chemical Sensors 2022 – Visegrád, Hungary, 2022.06.13. (2022. June 12-17., 2022)
- Po3 Anita, Bányai ; Petra, Hermann ; Orsolya, Hakkel ; Zoltán, Hajnal ; Péter, Fürjes; **Shape design dependent performance of DLD (deterministic lateral displacement) based particle separation systems - FEM modelling and validation** (2019) SelectBio, Lab-on-a-Chip and Microfluidics Europe 2019, Rotterdam 18-19.06.2019y.

## VIII. Additional scientific publications

---

### VIII.1 Publications

- P4 Farkas Enikő, Tarr Robert, Gerecsei Tamás, Saftics András, Kovács Kinga Dóra, Stercz Balázs, Domokos Judit, Péter Beatrix, Kurunczi Sándor, Székács Inna, Bonyár Attila, Bányai Anita, Fürjes Péter, Ruskai-Szaniszló Szilvia, Varga Máté, Szabó Barnabás, Ostorházi Eszter, Szabó Dóra, Horváth Róbert **Development and In-Depth Characterization of Bacteria Repellent and Bacteria Adhesive Antibody-Coated Surfaces Using Optical Waveguide Biosensing**, BIOSENSORS 12:2Paper:56,20p.(2022); <https://doi.org/10.3390/bios12020056>; Biosensors - Q1; IF 5.4; Number of references: 4 (Independent); 3 (Dependent)
- P5 Petrovszki, Dániel ✉; Valkai, Sándor; Gora, Evelin; Tanner, Martin; Bányai, Anita; Fürjes, Péter; Dér, András, **An integrated electro-optical biosensor system for rapid, low-cost detection of bacteria** MICROELECTRONIC ENGINEERING 239 Paper: 111523 , 9 p. (2021); <https://doi.org/10.1016/j.mee.2021.111523>; Microelectronic Engineering – Q2; IF 2.3; Number of references: 30 (Independent); 2 (Dependent)